1H NMR spectral analysis in series of heteroleptic triple-decker lanthanide phthalocyaninato complexes: Contact and dipolar contributions of lanthanide-induced shifts

ARTICLE *in* POLYHEDRON · JANUARY 2010

Impact Factor: 2.01 · DOI: 10.1016/j.poly.2009.06.009

2 AUTHORS:

Alexander G. Martynov
A. N. Frumkin Institute of Physical Chemistr…
26 PUBLICATIONS **203** CITATIONS
SEE PROFILE

Yu. G. Gorbunova
Russian Academy of Sciences
138 PUBLICATIONS **906** CITATIONS
SEE PROFILE

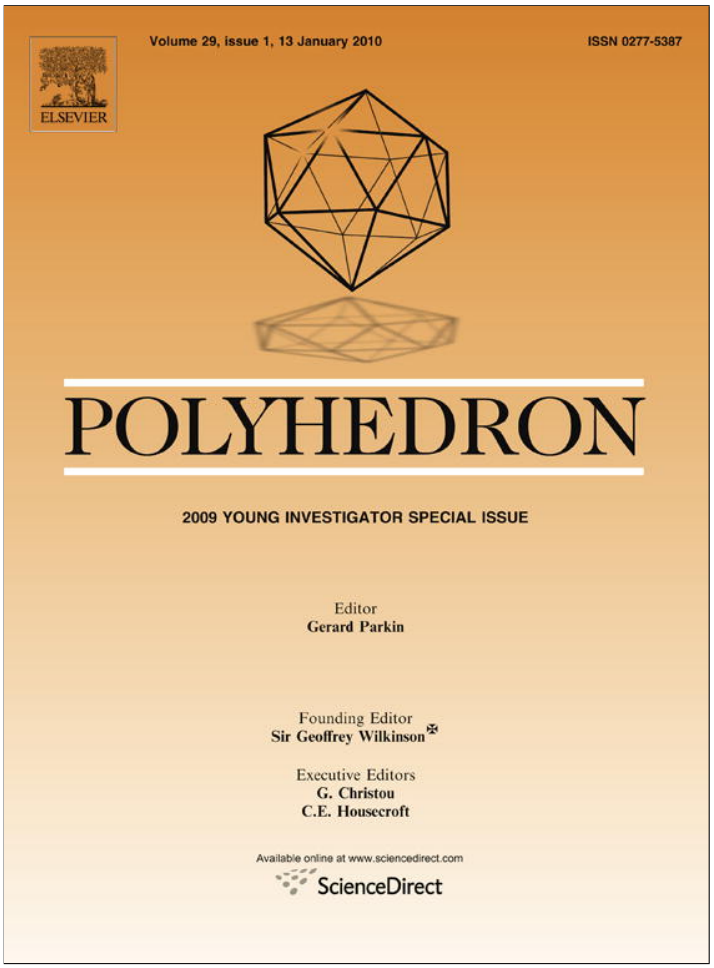

Polyhedron 29 (2010) 391–399

Contents lists available at ScienceDirect

Polyhedron

journal homepage: www.elsevier.com/locate/poly

^{1}H NMR spectral analysis in series of heteroleptic triple-decker lanthanide phthalocyaninato complexes: Contact and dipolar contributions of lanthanide-induced shifts

Alexander G. Martynov, Yulia G. Gorbunova *

A.N. Frumkin Institute of Physical Chemistry and Electrochemistry RAS, Leninsky Prosp. 31, Moscow 119991, Russia
N.S. Kurnakov Institute of General and Inorganic Chemistry RAS, Leninsky Prosp. 31, Moscow 119991, Russia

ARTICLE INFO

Article history:
Available online 10 June 2009

Keywords:
Heteroleptic phthalocyaninates
^{1}H NMR spectroscopy
Lanthanide-induced shift
Contact shift
Dipolar shift
Terbium

ABSTRACT

Model-free separation of lanthanide-induced shifts to contact and dipolar contributions was performed for the series of heteroleptic REE(III) trisphthalocyaninates, namely $[(15C5)_4Pc]M(Pc)M(Pc)$, where Pc^{2-} – phthalocyaninato-dianion, $[(15C5)_4Pc]^{2-}$ – 2,3,9,10,16,17,24,25-tetrakis(15-crown-5)phthalocyaninato-dianion, M = Nd, Sm, Eu, Tb, Dy, Er, Tm and Y as a diamagnetic reference. Application of one nucleus technique evidenced of abrupt changes of contact F_k and dipolar $A_2^0\langle r^2\rangle \cdot G_k$ terms between Tb and Dy. Not withstanding structural non-equivalence of lanthanide ions, they have virtually equal values of crystal-field parameters, which justified application of several crystal-field techniques for the further analysis of LIS data. Both two $(\Delta\delta_k/\langle S_Z\rangle_{Ln}; \Delta\delta_l/\langle S_Z\rangle_{Ln})$ and three nuclei $(\Delta\delta_k/\langle S_Z\rangle_{Ln}; \Delta\delta_l/\langle S_Z\rangle_{Ln}; \Delta\delta_m/\langle S_Z\rangle_{Ln})$ crystal-field independent graphical analysis evidenced of isostructurality of the complete series, therefore variation of solely $A_2^0\langle r^2\rangle$ between Tb and Dy was responsible for changes of dipolar terms. To study the behavior of contact terms, another three nuclei technique was firstly applied to lanthanide phthalocyaninates. Plotting $\Delta\delta_k/\Delta\delta_m$ versus $\Delta\delta_l/\Delta\delta_m$ demonstrated that in studied complexes F_k actually vary between Eu and Tb, therefore evidencing of non-simultaneous variations of contact and dipolar terms. Altogether, it let us refine the values of these terms, which would be subsequently applied for structural analysis of triple-decker crownphthalocyaninates and their supramolecular assemblies in solution.

1. Introduction

Specific structure of f-electronic shells of lanthanides gives rise to unique properties, which distinguish them from the rest of transition metals and affords numerous applications of these elements and their complexes [1]. One of these properties is significant shifting of resonance frequencies and enhancement of relaxation rates, which are observed in NMR spectra of paramagnetic lanthanides complexes in comparison with diamagnetic counterparts. Due to these properties, lanthanide complexes are widely used as shift reagents in NMR spectroscopy, contrast reagents in magnetic resonance imaging, structural probes in studies of chiral compounds, macromolecules and supramolecular assemblies [2]. Separation of lanthanide-induced shifts (LIS, $\Delta\delta_k$) to isotropic through-bond (Fermi or contact, $\Delta\delta_k^{con}$ [3]) and anisotropic through-space (dipolar or pseudocontact, $\Delta\delta_k^{dip}$ [4]) gives unique possibility to analyze the geometry of lanthanide complexes in solution, which is almost unavailable by other physical–chemical techniques. This aim can be achieved due to dependence of $\Delta\delta_k^{dip}$ on relative arrangement of the considered nucleus k and lanthanide ion.

Among lanthanide-containing compounds much attention is paid to their sandwich complexes with tetrapyrrolic ligands [5]. These compounds acquire specific features due to electronic π–π interaction between stacked ligands, which is governed by the size of metal center. The influence of interligand distance on optical and redox-features of these compounds was extensively investigated [6].

Much less papers are devoted to LIS analysis for series of sandwich lanthanide complexes with tetrapyrrolic compounds. Available information is scattered and suffers some inconsistencies. For example, Buchler et al. used ^{1}H NMR spectroscopy to study structure of dicerium(III) tris(octaethylpopthyrinate) in solution and revealed inter-ring steric crowding of alkyl groups, which leads to their limited rotation [7]. Konami et al. studied anionic forms or lanthanide bisphthalocyaninates $(Bu_4N^+)[Ln(Pc)_2]^-$ and demonstrated high symmetrical structure of anions in solution [8], however, there was much doubt about accuracy of NMR measurements [9]. As for lanthanide trisphthalocyaninates, these works are actually limited to studies of Arnold and Jiang [10] and also Ishikawa et al. [11]. The former group studied heteroleptic

* Corresponding author. Tel.: +7 495 9522566.
E-mail address: yulia@igic.ras.ru (Y.G. Gorbunova).

0277-5387/$ - see front matter © 2009 Elsevier Ltd. All rights reserved.
doi:10.1016/j.poly.2009.06.009

complexes (Pc)M[(OctO)$_8$Pc]M(Pc) and [(OctO)$_8$Pc]M[(OctO)$_8$Pc]M(Pc), where [(OctO)$_8$Pc] – octakis(*n*-octyloxy)phthalocyanine M = Y, Pr–Tm, except Pm and Gd [10]. The later group investigated homo- and heteronuclear complexes [(BuO)$_8$Pc]Ln(Pc)Ln(Pc), [(BuO)$_8$Pc]Y(Pc)Ln(Pc) and [(BuO)$_8$Pc]Ln(Pc)Y(Pc), where [(BuO)$_8$Pc] – octakis(*n*-butoxy)phthalocyaninate, Ln = Tb–Yb [11]. In spite of different initial assumptions and applied analytical methodologies, both groups concluded that complexes of each type are isostructural throughout lanthanide series; however the electronic features of lanthanide ions and therefore LIS characteristics are strongly lanthanide dependent. Both groups managed to obtain good correspondence between experimental and calculated LIS values, therefore resulting in two different explanations of LIS origin.

Recently, we have developed convenient synthetic approaches to several families of heteroleptic triple-decker crownphthalocyaninates with the application of lanthanide diphthalocyaninates as donors of phthalocyaninato-dianion. Reaction of tetra-15-crown-5-phthalocyanine, H$_2$[(15C5)$_4$Pc] (designated hereinafter as [Pc*]) with lanthanum diphthalocyaninate, La(Pc)$_2$ and REE(III) acetylacetonates in refluxing 1-chloronaphthalene, afforded two series of complexes – (Pc)M[Pc*]M(Pc) and [Pc*]M[Pc*]M(Pc), M = Nd, Sm, Eu, Tb, Dy, Tm, Y [12]. Application in the same reaction of more stable diphthalocyaninates, M(Pc)$_2$ gave the complexes [Pc*]M(Pc)M(Pc) [13]. Particular interest to crown-substituted phthalocyaninates can be explained by the possibility to control their supramolecular assembling by addition of alkali–metal ions [13,14], which makes them perfect candidates to elaboration of molecular functional devices on their basis [15]. From this viewpoint, structural investigation of building blocks based on analysis of LIS, can give significant insight into architecture of supramolecular assembles, formed by these compounds in solution. Furthermore, analysis of LIS can also reveal correlation between chemical structure of complexes and their magnetic properties; it is of further consequence for development of molecular magnetic materials [11].

In order to reveal ^{1}H NMR spectral–structural correlations in series of lanthanide crownphthalocyaninates and their supramolecular aggregates, we report here analysis of LIS for protons of aromatic core of complexes [Pc*]M(Pc)M(Pc) (Fig. 1) in terms of contact and dipolar contributions by various model-free methods. The choice of this family of complexes is explained mostly by that fact that it contains maximum number of non-equivalent aromatic protons among other triple-decker crownphthalocyaninates, so its investigation should give maximum amount of information about electronic and geometrical characteristics of lanthanide triple-decker complexes.

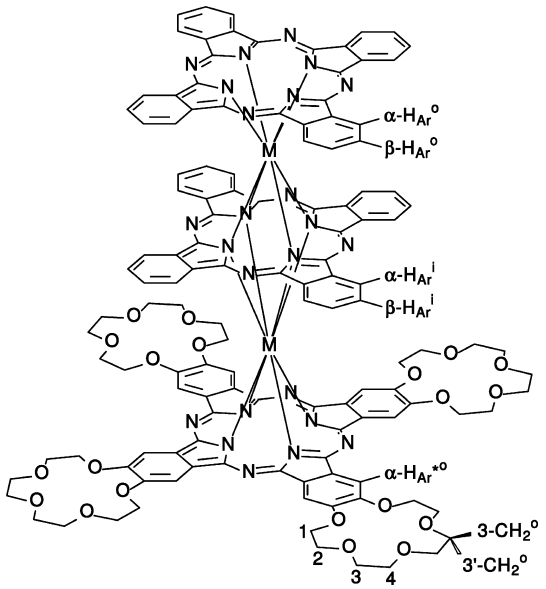

Fig. 1. Chemical structure and designation of protons applied in assignment of ^{1}H NMR spectra of [Pc*]M(Pc)M(Pc).

2. Experimental

The compounds [Pc*]M(Pc)M(Pc), M = Nd, Sm, Eu, Tb, Dy, Er Tm and Y were synthesized as reported previously [13]. ^{1}H NMR spectra were recorded on Bruker Avance-400 (400 MHz) in $CDCl_3$ solution in the presence of 10 μl of 1% solution of $N_2H_4{\cdot}H_2O$ in methanol-[d_4]. Chemical shifts were reported as the δ [ppm] relative to internal standard (residual $CHCl_3$, δ = 7.25 ppm) at T = 298 K. Designation of protons, used for assignment of NMR spectra is given in Fig. 1. Regression analysis was made with the application of ORIGIN 7.5 and SIGMAPLOT 11.0 software. Complete NMR data are given in Supplementary data available online.

3. Results and discussion

3.1. Assignment of resonance signals in ^{1}H NMR spectra of [Pc*]M(Pc)M(Pc)

Resonance signals of five types of aromatic protons and four pairs of *exo*- and *endo*-CH_2 protons (altogether, 13 signals) with equal integral intensities are observed in ^{1}H NMR spectra of [Pc*]M(Pc)M(Pc) [13].

Assignment of signals in the spectrum of diamagnetic yttrium complex was achieved with the application of ^{1}H–^{1}H COSY technique, which revealed spin–spin coupling between pairs of α- and β-aromatic protons in inner and outer unsubstituted ligands. However, this technique is useless in the case of strongly paramagnetic complexes which are characterized by very high relaxation rates. This limitation can be overcome due to the strong predominance of dipolar contribution in LIS values in triple-decker phthalocyaninates. It justifies the application of simple geometrical consideration: the smaller is the distance between paramagnetic centers and proton, the larger is the LIS value. Previously application of this approach afforded complete assignment of ^{1}H NMR spectra of Dy and Tm complexes, which exhibit very large LIS values (up to −81 and +43 ppm, respectively for α-H$^i_{Ar}$ [13]). The same approach was used herein for the analysis of spectra of Tb and Er complexes (LIS of α-H$^i_{Ar}$ is −158 and +36 ppm, respectively).

Neodymium and europium are characterized by smaller LIS, thus assignment of resonance signals other then for α-H$^i_{Ar}$, which still should suffer the largest LIS, becomes more ambiguous. For the complete assignment, we developed the method, which is based on the virtual invariance of relative LIS values (RLIS) throughout the series of investigated complexes [11]. For two protons k and l RLIS can be evaluated as

$$\mathrm{RLIS}(\mathrm{H}_k, \mathrm{H}_l) = \frac{\Delta\delta_k}{\Delta\delta_l} = \frac{\delta_k^{\mathrm{Ln}} - \delta_k^{\mathrm{Y}}}{\delta_l^{\mathrm{Ln}} - \delta_l^{\mathrm{Y}}} \quad (1)$$

Since α-H$^i_{Ar}$ is the only type of protons, for which assignment is still quite evident, its resonance signal was used as a reference $\Delta\delta_l$ to give the following equation:

$$\delta_k^{\mathrm{Ln}} = \delta_k^{\mathrm{Y}} + \mathrm{RLIS}(H_k, \alpha\text{-H}^{\mathrm{i}}_{\mathrm{Ar}}) \cdot \Delta\delta(\alpha\text{-H}^{\mathrm{i}}_{\mathrm{Ar}}) \quad (2)$$

Values RLIS(H_k, α-H$^i_{Ar}$) are available from our previous studies of Sm, Dy and Tm complexes together with data, reported herein for Tb and Er complexes. Positions of resonance signals for yttrium complexes are also determined. Thus, to apply Eq. (2) to Nd and

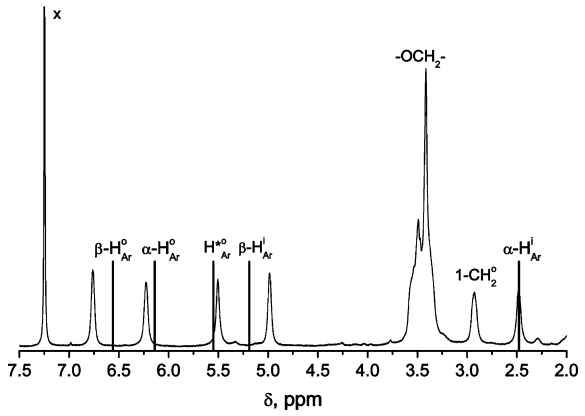

Fig. 2. Experimental (solid line) and simulated with the application of Eq. (2) (vertical lines) ^{1}H NMR spectra of [Pc*]Nd(Pc)Nd(Pc) in $CDCl_3$ (x – signal of residual $CHCl_3$).

Eu complexes it is only needed to substitute respective values for certain proton together with $\Delta\delta^{Ln}(\alpha\text{-}H^i_{Ar})$. This procedure gives approximate positions of resonance signals which are fairly close to their positions in experimental ^{1}H NMR spectra (Fig. 2). It can be seen that Nd and Eu complexes have different order of resonance signals while moving from upfield to downfield region, however $\Delta\delta$ values decrease in the same sequence as the distance between considered proton and paramagnetic nuclei. Complete set of resonance signals of aromatic protons is given in Table 1.

Assignment of resonance signals of crown-ether aliphatic protons for the "light" lanthanides is more complicated since they are remote from paramagnetic centers and in the case of metals with small LIS (Nd, Sm, Eu) overlapping multiplets are observed instead of distinct signals in spectra of Tb, Dy, Er and Tm complexes. Simulation of resonance signal positions can also be made for these elements. Yet, it gives less information for the assignment of signals, especially in the case of Nd complex, which exhibit broad and almost unstructured signal in the region 3.2–3.7 ppm (Fig. 2). Therefore, the data for crown-ether protons would not be considered in the present investigation.

3.2. One nucleus analysis of [Pc*]M(Pc)M(Pc): separation of lanthanide-induced shifts to contact and dipolar contributions

Lanthanide-induces shift depends both on the nature of Ln^{3+} and on the relative position of Ln^{3+} ions and concerned atom. In the general case, the expression for LIS is a power series of T^{-n}, reciprocal of temperature, which also includes several terms, which depend on polar coordinates of resonating nucleus in arbitrary Cartesian frame. Altogether it results in cumbersome equation, which is not well suited for analysis of experimental data [16]. In the case of axial symmetry of complexes (at least C_3), in terms of Bleaney high-temperature expansion (terms depending on T^{-n}, $n > 2$ are neglected [4b]), LIS expression is simplified, giving

$$\Delta\delta_k = \Delta\delta_k^{con} + \Delta\delta_k^{dip} = \langle S_Z\rangle_{Ln}\cdot F_k + C_{Ln}\cdot A_2^0\langle r^2\rangle\cdot G_k \quad (3)$$

where F_k is the hyperfine electron-nuclear coupling constant of resonating nucleus k and Ln^{3+}, $\langle S_Z\rangle_{Ln}$ – the spin expectation value of Ln^{3+} [3], C_{Ln} – the characteristic for Ln^{3+} value proportional to Bleaney's factor [4b,c], $A_2^0\langle r^2\rangle$ is the second-rank crystal-field parameter, which characterizes the magnitude of metal–ligand interaction in the considered complexes. The term $G_k = l^{-3}(3\cos^2\theta - 1)$ is the geometrical function, which is specified by the azimuth θ and the distance l of the resonating nucleus k in the principal magnetic axes system with Ln^{3+} in the origin. Typically, contact contribution has relatively small value in comparison with dipolar one. Moreover, it decreases strongly with the increase of number of chemical bonds which separates nucleus and Ln^{3+} ion. However, $\Delta\delta^{con}$ should not be neglected, especially in the case of "heavy" lanthanides, since its value is amplified by large values of $\langle S_Z\rangle_{Ln}$.

Extraction of $\Delta\delta^{dip}$ is required to perform structural analysis [2]. This is usually achieved by rearrangement of Eq. (3), firstly proposed by Reilley et al. [17]. It results in the following linear form:

$$\frac{\Delta\delta_k}{\langle S_Z\rangle_{Ln}} = F_k + \frac{C_{Ln}}{\langle S_Z\rangle_{Ln}}\cdot A_2^0\langle r^2\rangle\cdot G_k \quad (4)$$

According to Eq. (4) the plot $C_{Ln}/\langle S_Z\rangle_{Ln}$ versus $\Delta\delta_k/\langle S_Z\rangle_{Ln}$ should give a straight line with the slope $A_2^0\langle r^2\rangle\cdot G_k$ and intercept F_k throughout the series of isostructural complexes. But in practice such plots usually demonstrate breaks near the middle of lanthanide series – the so called "gadolinium breaks" [18]. These breaks can be explained by changes of electronic characteristics F_k and $A_2^0\langle r^2\rangle$ and/or structural variations associated with lanthanide contraction [19,20].

Eqs. (3) and (4) are also applicable in the case of multinuclear systems with several paramagnetic lanthanides due to additive property of LIS. The presence of several paramagnetic nuclei in the molecule doesn't affect the methods of analysis, but it should be kept in mind that in this case the resulting F_k and G_k are actually the sums of contributions from each lanthanide. The additivity of LIS was successfully checked on several examples (for instance, polynuclear supramolecular helicates [20], homo- and heteronuclear complexes with 1,3,5-triamino-1,3,5-tridesoxy-*cis*-inositol [21], triple-decker porphyrinates [7] and phthalocyaninates [10,11]).

Studied herein complexes contain two lanthanide ions in different coordination surrounding, namely one of them is sandwiched between two unsubstituted Pc rings, and one – between Pc and [(15C5)$_4$Pc]. X-ray studies of structurally similar heteroleptic trisphthalocyaninate [(α-$C_5H_{11}O)_4$Pc]M(Pc)M(Pc), M = Gd, Lu [22] revealed slight difference in M–N bonds length for two different lanthanide ions. Altogether, this can result in non-equivalence of crystal-field coefficients $A_2^0\langle r^2\rangle$. Since dipolar term, obtained by treating of experimental data with the application of Eq. (4) is a sum of two contributions, it would be further designated by superscript "Σ". The same designation would be applied for contact term F_k:

$$^{\Sigma}F_k = F_k^{Ln1} + F_k^{Ln2}$$

$$^{\Sigma}A_2^0\langle r^2\rangle\cdot G_k = A_2^0\langle r^2\rangle^{Ln1}\cdot G_k^{Ln1} + A_2^0\langle r^2\rangle^{Ln2}\cdot G_k^{Ln2}$$

Before discussing the results of one nucleus analysis of [Pc*]M(Pc)M(Pc), it should be specially mentioned, that the applied tabular parameters, namely $\langle S_Z\rangle_{Ln}$, are available from studies, reported by different groups. Generally, these terms have almost identical values for all lanthanides. The major uncertainty is related to Sm and Eu due to stronger dependency of their spin expec-

Table 1
Assignment or resonance signals of aromatic protons in ^{1}H NMR spectra of [Pc*]M(Pc)M(Pc) in $CDCl_3$ at 298 K.

Proton	δ (ppm)							
	Nd	Sm	Eu	Tb	Dy	Er	Tm	Y
α-H^i_{Ar}	2.48	7.39	13.13	−148.51	−72.05	45.10	54.40	8.97
β-H^i_{Ar}	4.99	7.85	11.37	−76.35	−34.37	28.86	33.56	8.71
H^{*o}_{Ar}	5.51	7.30	9.27	−54.81	−24.00	22.64	26.14	7.86
α-H^o_{Ar}	6.23	7.87	9.80	−53.27	−24.00	22.17	26.14	8.44
β-H^o_{Ar}	6.76	7.72	8.70	−31.67	−12.78	15.41	18.70	8.09

tation values both on coordination surrounding and temperature in comparison with other lanthanides [3]. Initially, these values were calculated by Golding and Halton in 1972 [3a]. In 13 years Pinkerton et al. refined these terms by means of analysis of ^1H and ^{31}P NMR spectra of $[Ln(S_2PR_2)_4]^-$ [3b]. This investigation leaded to almost 4 times increase of $\langle S_Z\rangle_{Sm}$ in comparison with the value, reported by Golding and Halton (0.224 versus 0.063). The value $\langle S_Z\rangle_{Eu}$ was also corrected, but it did not suffer much variation (7.57 versus 10.68). Spin expectation values for other elements remained almost unchanged.

The analysis of available reported data evidences that both sets of $\langle S_Z\rangle_{Ln}$ were successfully used in order to separate LIS to contact and dipolar contributions [2a]. However, data for Sm usually was not considered, therefore the problem with the uncertainty of its spin expectation value simply didn't arise. In the present case we did not discard data for Sm with the aim to determine the applicable set of $\langle S_Z\rangle_{Ln}$ terms. The applicability was investigated by simulation of LIS values with the found $^{\Sigma}F_k$ and $^{\Sigma}A_2^0\langle r^2\rangle\cdot G_k$ and subsequent measuring of Willcott agreement factors AF_k [23] between calculated ($\Delta\delta^{calc}_{k,Ln}$) and observed ($\Delta\delta^{obs}_{k,Ln}$) LIS for each proton (Eq. (5), Table 2).

$$AF_k=\sqrt{\frac{\sum_{Ln}\left(\Delta\delta^{obs}_{k,Ln}-\Delta\delta^{calc}_{k,Ln}\right)^2}{\sum_{Ln}\left(\Delta\delta^{obs}_{k,Ln}\right)^2}} \tag{5}$$

One more indicator of simulation quality was found via plotting the simulated LIS versus experimental ones. Linear regression of the obtained array results in the line defined by the equation $\Delta\delta^{calc}=A\cdot\Delta\delta^{obs}+B$ and characterized by its own correlation coefficient R^2 [17b]. The closer are A and R^2 to one and B – to zero, the better is the quality of simulation.

Analysis of LIS data for the series of [Pc*]M(Pc)M(Pc) in accordance with Eq. (4) systematically reveals breaks in the plots $C_{Ln}/\langle S_Z\rangle_{Ln}$ versus $\Delta\delta_k/\langle S_Z\rangle_{Ln}$ near the middle of lanthanide series (Fig. 3), which separate these elements into two subfamilies. It indicates that both $^{\Sigma}F_k$ and $^{\Sigma}A_2^0\langle r^2\rangle\cdot G_k$ undergo abrupt changes along lanthanides, however each subfamily has constant values of these terms.

Least squares method was applied to find $^{\Sigma}F_k$ and $^{\Sigma}A_2^0\langle r^2\rangle\cdot G_k$ for two different partitions of lanthanides, conveniently designated hereinafter as (Nd–Tb)(Dy–Tm) and (Nd–Eu)(Tb–Tm) to determine the exact position of the border between subfamilies and to investigate the behavior of contact and dipolar terms in each subfamily.

Application of the parameters $\langle S_Z\rangle_{Ln}$ proposed by Golding and Halton [3a] for the simulation of LIS evidences of overestimation of calculated LIS (A = 1.23) in subfamily (Nd–Tb), while removal of Tb from this subfamily results in decrease of A to the value of 0.95. To the contrast, application of corrected values of $\langle S_Z\rangle_{Ln}$ afforded by Pinkerton et al. [3b] results in high conformity between calculated and simulated data for both subfamilies – (Nd–Tb) and (Nd–Eu) ($A^{Nd-Tb}=1.05$ and $A^{Nd-Eu}=1.01$, $R^2>0.99$ in both cases). Therefore, all subsequent calculations will be performed with these values. The list of calculated contact and dipolar terms for both partitions is given in Table 2.

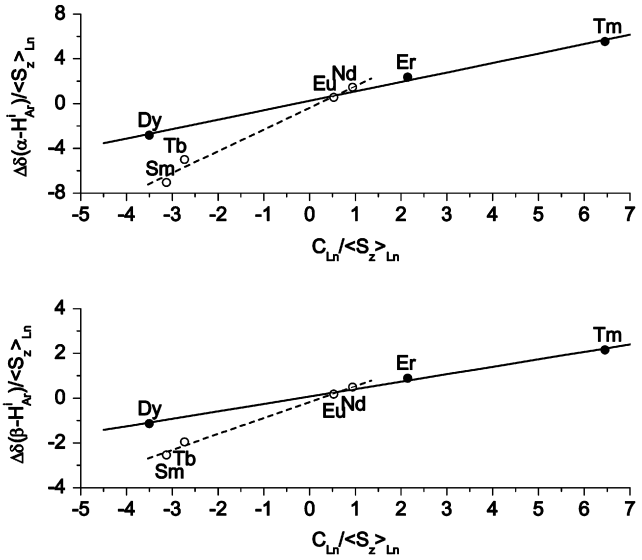

Fig. 3. Plots $C_{Ln}/\langle S_Z\rangle_{Ln}$ versus $\Delta\delta_k/\langle S_Z\rangle_{Ln}$ for α-H^i_{Ar} (top) and α-H^o_{Ar} (bottom), $CDCl_3$, 298 K.

Data, given in Table 2 demonstrates that addition of Tb to this or that subfamily strongly influences the quality of fitting. Addition of Tb to "heavy" lanthanides significantly decreases R^2 and increases AF_k, while exclusion of Tb from this group results in satisfactory values of correlation indicators. The same is true for the "light" lanthanides: subfamily (Nd–Tb) is characterized by higher values of AF_k in comparison with (Nd–Eu), though in the present case the increase of AF_k is not so dramatic.

It can be seen that dipolar terms $^{\Sigma}A_2^0\langle r^2\rangle\cdot G_k$ are not very sensitive to inclusion of Tb to "light" lanthanides, while contact terms $^{\Sigma}F_k$ suffer drastic perturbations upon addition of Tb to this group. In the case of the "heavy" group addition of Tb even leads to change of the sign of $^{\Sigma}F_k$ which generally results in strong increase of AF_k. The correlation between calculated and observed LIS within (Tb–Tm) is very poor (A = 0.81, R^2 = 0.8600), while (Dy–Tm) is characterized by perfect agreement (A = 1.00, R^2 = 0.9952).

Altogether, the obtained sets of parameters evidence, that the border between lanthanides, which determine the abrupt changes of contact and dipolar terms, is likely to be placed between Tb and

Table 2
Calculated values of contact $^{\Sigma}F_k$ and dipolar $^{\Sigma}A_2^0\langle r^2\rangle\cdot G_k$ terms and agreement factors for aromatic protons of [Pc*]Ln(Pc)Ln(Pc) ($CDCl_3$, 298 K).

Nuclei	$^{\Sigma}A_2^0\langle r^2\rangle\cdot G_k$	$^{\Sigma}F_k$	R^2	AF_k	$^{\Sigma}A_2^0\langle r^2\rangle\cdot G_k$	$^{\Sigma}F_k$	R^2	AF_k
	(Nd–Eu)				(Nd–Tb)			
α-H^i_{Ar}	2.088	−0.532	1.0000	0.02	1.940	−0.386	0.9838	0.14
β-H^i_{Ar}	1.148	−0.251	1.0000	0.01	1.066	-0.170	0.9838	0.14
H^{*o}_{Ar}	0.741	−0.187	0.9999	0.06	0.714	−0.161	0.9961	0.06
α-H^o_{Ar}	0.747	−0.211	1.0000	0.01	0.712	−0.177	0.9932	0.08
β-H^o_{Ar}	0.477	−0.161	0.9999	0.06	0.453	−0.137	0.9919	0.09
	(Tb–Tm)				(Dy–Tm)			
α-H^i_{Ar}	0.996	−0.578	0.9258	0.35	0.845	0.246	0.9964	0.09
β-H^i_{Ar}	0.541	−0.288	0.9241	0.36	0.458	0.165	0.9962	0.11
H^{*o}_{Ar}	0.398	−0.215	0.9245	0.36	0.337	0.117	0.9962	0.10
α-H^o_{Ar}	0.390	−0.243	0.9290	0.34	0.332	0.073	0.9969	0.07
β-H^o_{Ar}	0.240	−0.198	0.9275	0.34	0.204	−0.0005	0.9989	0.03

Dy, notwithstanding some notable decrease of fitting quality when Tb is treated as "light" lanthanide.

3.3. Checking of isostructurality of [Pc*]M(Pc)M(Pc) along lanthanide series

Since in the absence of adequate structural model (X-ray, quantum-chemical calculations or both) separation of $^{\Sigma}A_2^0\langle r^2\rangle \cdot G_k$ into individual multipliers is impossible, the variation of the slope in the described above one nucleus plot may evidence either of structural variations along the series due to lanthanide contraction or of solely variation of $A_2^0\langle r^2\rangle$ with almost constant geometry of compounds. To eliminate the crystal-field parameter from Eq. (4), and therefore to check the continuity of G_k, LIS of two protons should be considered. The most common method which is applied for this purpose was proposed by Reuben [24] and further modified by Geraldes [2f,25]. It is based on expression of $C_{\mathrm{Ln}} \cdot A_2^0\langle r^2\rangle$ from Eq. (1) written for nucleus k and substitution of this term to the same equation for another nucleus l, which results in reduction of crystal-field parameter, yielding

$$\frac{\Delta\delta_k}{\langle S_Z\rangle_{\mathrm{Ln}}} = \left(F_k - F_l \cdot \frac{G_k}{G_l}\right) + \frac{G_k}{G_l} \cdot \frac{\Delta\delta_l}{\langle S_Z\rangle_{\mathrm{Ln}}} = (F_k - F_l \cdot R_{kl}) + R_{kl} \cdot \frac{\Delta\delta_l}{\langle S_Z\rangle_{\mathrm{Ln}}} \quad (6)$$

In the case of polynuclear compounds with equivalent lanthanide ions the observed slope would be a ratio of two sums of geometrical parameters

$$^{\Sigma}R_{kl} = \frac{G_k^{\mathrm{Ln1}} + G_k^{\mathrm{Ln2}}}{G_l^{\mathrm{Ln1}} + G_l^{\mathrm{Ln2}}}$$

Generally speaking, in the case of [Pc*]M(Pc)M(Pc) Eq. (6) can be inappropriate because of the presence of two non-equivalent lanthanide ions in the molecule. For this reason, algebraic transformations which were applied to get Eq. (6), would not afford removal of crystal-field parameters and the slope of least-squares line would still depend both on $A_2^0\langle r^2\rangle$ and G_k. Elimination of crystal-field parameter in polynuclear compounds (both axial and rhombic) was achieved by Piguet et al. [20c,21] via simultaneous treatment of data for three protons. Solving the system of two algebraic Eqs. (4) written for the pair of protons located in the framework of two lanthanide ions (Fig. 4) gives the expressions for two crystal-field parameters $A_2^0\langle r^2\rangle^{\mathrm{Ln1}}$ and $A_2^0\langle r^2\rangle^{\mathrm{Ln2}}$. Substitution of these parameters in Eq. (4) written for the third proton results in Eqs. (7)–(10), which defines the plane, separated by B_{klm} from the origin.

$$\frac{\Delta\delta_m}{\langle S_Z\rangle_{\mathrm{Ln}}} = B_{klm} + C_{klm}\frac{\Delta\delta_k}{\langle S_Z\rangle_{\mathrm{Ln}}} + D_{klm}\frac{\Delta\delta_l}{\langle S_Z\rangle_{\mathrm{Ln}}} \quad (7)$$

$$B_{klm} = F_m - F_k \cdot C_{klm} - F_l \cdot D_{klm} \quad (8)$$

$$C_{klm} = \frac{G_l^{\mathrm{Ln2}} \cdot G_m^{\mathrm{Ln1}} - G_l^{\mathrm{Ln1}} \cdot G_m^{\mathrm{Ln2}}}{G_k^{\mathrm{Ln1}} \cdot G_l^{\mathrm{Ln2}} - G_k^{\mathrm{Ln2}} \cdot G_l^{\mathrm{Ln1}}} \quad (9)$$

$$D_{klm} = \frac{G_k^{\mathrm{Ln2}} \cdot G_m^{\mathrm{Ln1}} - G_k^{\mathrm{Ln1}} \cdot G_m^{\mathrm{Ln2}}}{G_k^{\mathrm{Ln1}} \cdot G_l^{\mathrm{Ln2}} - G_k^{\mathrm{Ln2}} \cdot G_l^{\mathrm{Ln1}}} \quad (10)$$

The coefficients C_{klm} and D_{klm} which define the position of best plane in 3D space depend solely on geometrical parameters of protons; therefore, any discontinuity of these parameters should reveal abrupt structural variations along lanthanide series.

To perform the analysis, five types of aromatic protons were arbitrarily assigned in the following manner: 1 – α-H^{i}_{Ar}, 2 – β-H^{i}_{Ar}, 3 – H^{*o}_{Ar}, 4 – α-H^{o}_{Ar}, 5 – β-H^{o}_{Ar}. The selection rules $k \neq l \neq m$ and $k < l < m$ gave finally 10 possible "*klm*" combinations of five elements. The quality of fitting was measured by average agreement factor AF_{klm} [20c,21]. Performing this analysis for different triads "*klm*" of aromatic protons in [Pc*]M(Pc)M(Pc) did not reveal any discontinuity and all experimental points within each triad were sharing the same plane with average agreement factors AF_{klm} in the interval $7.97 \times 10^{-3} \div 1.65 \times 10^{-2}$ (Fig. 5). Obtained results evidence of isostructurality of complexes along lanthanide series, but nonlinear character of regression coefficients B_{klm}, C_{klm} and D_{klm} makes it difficult to determine structural features of complexes in solution.

Analysis of scattering of experimental points in 3D space revealed that each studied triad the points form lines rather then planes (Fig. 5). Their linear distribution becomes more evident when the projections on *xy*-, *xz*- and *yz*-coordination planes are examined. Each of these projections is a plot built in coordinates $\Delta\delta_l/\langle S_Z\rangle_{\mathrm{Ln}}$ versus $\Delta\delta_k/\langle S_Z\rangle_{\mathrm{Ln}}$. In all studied cases these plots did not reveal any significant discontinuity (Fig. 5). In accordance with Eq. (6) such plots are linear for the series of isostructural compounds, which contain one or several equivalent lanthanide ions. Thus, it seems attractive to associate linearity of 3D-plots and their 2D projections obtained for binuclear [Pc*]M(Pc)M(Pc) with isostructurality of these compounds. To make such an association and, therefore, to justify the application of Eq. (6), the equivalence of $A_2^0\langle r^2\rangle^{\mathrm{Ln1}}$ and $A_2^0\langle r^2\rangle^{\mathrm{Ln2}}$ should be proved.

Previously, Ishikawa et al. studied crystal-field parameters in heteroleptic heteronuclear triple-decker [(BuO)$_8$Pc]Y(Pc)Ln(Pc) and [(BuO)$_8$Pc]Ln(Pc)Y(Pc) via simultaneous NMR and magnetic susceptibility measurements and determined high-order crystal-field parameters $A_2^0\langle r^2\rangle$, $A_4^0\langle r^4\rangle$, $A_4^4\langle r^4\rangle$, $A_6^0\langle r^6\rangle$ and $A_4^4\langle r^6\rangle$ [11]. Comparison of the obtained sets of $A_2^0\langle r^2\rangle$ for both series of complexes reveals that these parameters are almost insensitive to their coordination surrounding, namely location between unsubstituted or BuO-substituted Pc ligands. For example, in the case of Tb second-rank terms are equal to 289.4 and 292.8 cm^{-1}, respectively [11]. The authors demonstrated that at room temperature coupling between paramagnetic sites is negligible, thus ^{1}H NMR spectra of homonuclear triple-decker complexes can be regarded as a superposition of two heteronuclear counterparts [11c].

Since four crown-ether groups, fused to terminal Pc ligand in the case of [Pc*]M(Pc)M(Pc) are similar to eight BuO-groups in [(BuO)$_8$Pc]M(Pc)M(Pc), we can assume that in the studied herein series of complexes $A_2^0\langle r^2\rangle^{\mathrm{Ln1}}$ and $A_2^0\langle r^2\rangle^{\mathrm{Ln2}}$ can be treated as equal, therefore application of Eq. (6) for analysis of heteroleptic trisphthalocyaninates is valid.

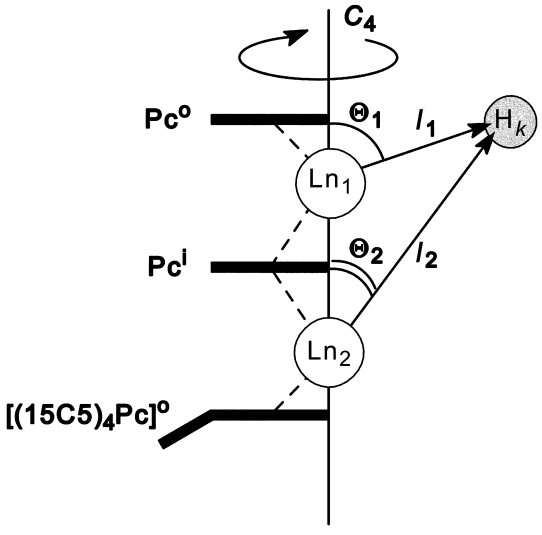

Fig. 4. Polar frame, formed by two non-equivalent paramagnetic lanthanide ions in [Pc*]M(Pc)M(Pc).

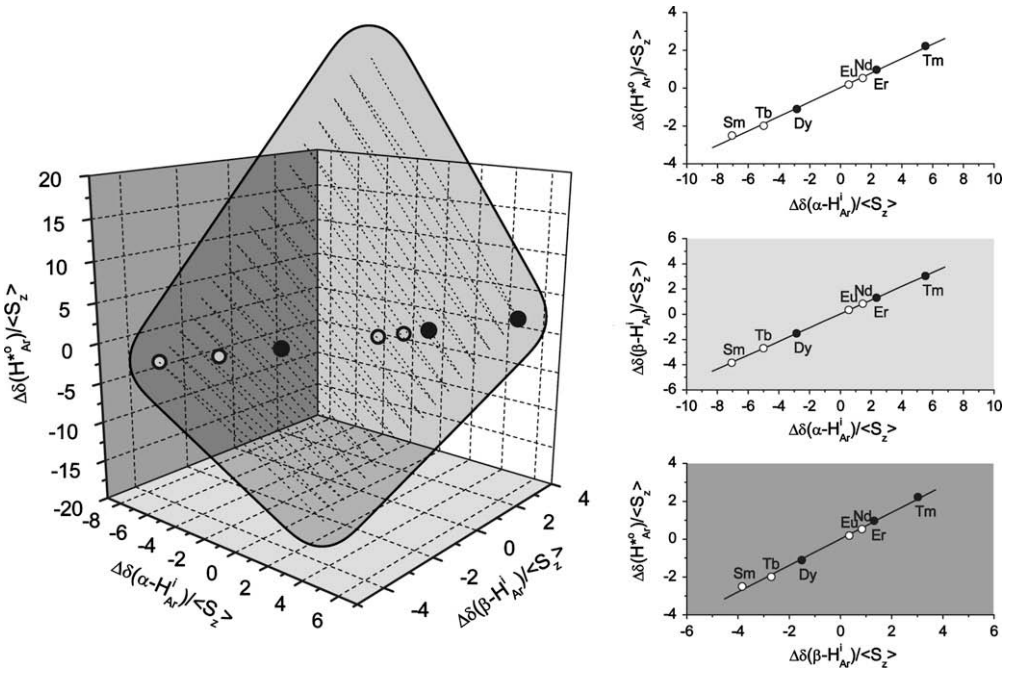

Fig. 5. 3D plot $\left(\frac{\Delta\delta(\alpha\text{-}H^{i}_{Ar})}{\langle S_Z\rangle};\frac{\Delta\delta(\beta\text{-}H^{i}_{Ar})}{\langle S_Z\rangle};\frac{\Delta\delta(H^{*o}_{Ar})}{\langle S_Z\rangle}\right)$ and its projections onto coordinate *xy*-, *xz*- and *yz*-planes. Open circles define Nd–Tb subfamily and closed Tb–Tm group.

Table 3 contains examples of least-squares regression analysis performed to find coefficients of Eq. (6) for four pairs of protons. All other possible ratios can be expressed as linear combinations of these four values. The observed linearity indicates that all ${}^{\Sigma}G_k$ values have almost constant values and, therefore, all complexes [Pc*]M(Pc)M(Pc) are isostructural throughout lanthanide series. In turn, it evidences that the abrupt change of ${}^{\Sigma}A_2^0\langle r^2\rangle \cdot G_k$ is due to variation of ligand field parameters $A_2^0\langle r^2\rangle$ rather then geometrical factors ${}^{\Sigma}G_k$.

The obtained ratios of geometrical parameters ${}^{\Sigma}R_{kl}$ are very close to the previously found average relative LIS values [13], which were used herein for the assignment of ^{1}H NMR spectra of synthesized triple-decker complexes via Eq. (2). The alternative way to get these RLIS is plotting $\Delta\delta_k$ versus $\Delta\delta_l$. Notwithstanding this method completely neglects contact contributions to LIS, this procedure resulted in perfect linear correlations with $R^2 > 0.99$ and slope coefficients fairly close to ${}^{\Sigma}R_{kl}$ found via plotting $\Delta\delta_l/\langle S_Z\rangle_{Ln}$ versus $\Delta\delta_k/\langle S_Z\rangle_{Ln}$. Good correspondence between these results justifies the application of Eq. (2) for assignment of NMR spectra of compounds with the predominance of dipolar contribution.

The ratio ${}^{\Sigma}R_{kl}$ can be also simulated using the results of one nucleus analysis since each proton in each subfamily is characterized by its own ${}^{\Sigma}A_2^0\langle r^2\rangle \cdot G_k$ term. Taking these terms for any pair of protons k and l and dividing them one by another gives ${}^{\Sigma}R_{kl}$ for both series (Table 3). It can be seen that $({}^{\Sigma}R_{kl})^{obs}_{Nd-Tm}$ have intermediate values between corresponding $({}^{\Sigma}R_{kl})^{obs}_{Nd-Tb}$ and $({}^{\Sigma}R_{kl})^{obs}_{Dy-Tm}$. The difference between simulated values $({}^{\Sigma}R_{kl})^{obs}_{Nd-Tb}$ and $({}^{\Sigma}R_{kl})^{obs}_{Dy-Tm}$ is likely to reflect minor geometrical changes of sandwich complexes associated with lanthanide contraction (decrease of interligand distance and increase of ligand deformation [26]). Nevertheless, these changes are still not significant to give any measurable break in two nuclei plot. Actually, splitting data to two groups – (Nd–Tb) and (Dy–Tm), and individual treating of each group by two nuclei technique gave exactly the same ratios as the values, found from one nucleus simulation for each subfamily. But in the absence of the results of one nucleus analysis this splitting seems to be speculative, because there is no significant difference between regression coefficients, which characterize these subfamilies.

The ratio of $A_2^0\langle r^2\rangle$ for two different subfamilies can be found by plotting $({}^{\Sigma}A_2^0\langle r^2\rangle \cdot G_k)_{Nd-Tb}$ versus $({}^{\Sigma}A_2^0\langle r^2\rangle \cdot G_k)_{Dy-Tm}$. This procedure gives the straight line with the slope 2.36 and regression coefficient R^2 0.9976. While G_k is almost constant along the lanthanide series, the obtained slope is equal to the ratio $(A_2^0\langle r^2\rangle \cdot G_k)_{Nd-Tb}/(A_2^0\langle r^2\rangle \cdot G_k)_{Dy-Tm}$, evidencing of more than two-times decrease of crystal-field parameter when going from "light" to "heavy" lanthanides due to weakening of metal–ligand interactions because of lanthanide contraction.

Table 3
Comparison of geometrical ratios ${}^{\Sigma}R_{kl}$ found by two nuclei technique, simulation with data, available from one nucleus analysis and relative LIS.

Term	β-H^{i}_{Ar}	H^{*o}_{Ar}	α-H^{o}_{Ar}	β-H^{o}_{Ar}
$({}^{\Sigma}R_{kl})^{obs}_{Nd-Tm}$	0.546	0.382	0.377	0.235
$({}^{\Sigma}F_k - {}^{\Sigma}F_l{}^{\Sigma}R_{kl})^{obs}_{Nd-Tm}$	0.0293	0.0294	-0.0040	-0.0458
R^2	1.0000	0.9967	0.9981	0.9989
$({}^{\Sigma}R_{kl})^{obs}_{Nd-Tb}$	0.549	0.368	0.367	0.234
$({}^{\Sigma}F_k - {}^{\Sigma}F_l{}^{\Sigma}R_{kl})^{obs}_{Nd-Tb}$	0.042	-0.019	-0.035	-0.047
$({}^{\Sigma}R_{kl})^{obs}_{Dy-Tm}$	0.543	0.400	0.392	0.241
$({}^{\Sigma}F_k - {}^{\Sigma}F_l{}^{\Sigma}R_{kl})^{obs}_{Dy-Tm}$	0.031	0.019	-0.024	-0.060
RLIS(H_k, α-H^{i}_{Ar})	0.541	0.398	0.392	0.248

3.4. Behavior of contact term in series of [Pc*]M(Pc)M(Pc)

To get further insight into the behavior of contact and dipolar terms, we have used the tree nuclei method, suggested by Geraldes et al. [2f,27].

This method is completely empirical and it gives the possibility to check invariance of hyperfine coupling and geometrical constants by plotting one ratio of LIS versus another one in accordance with Eqs. (11)–(13). This method doesn't require any tabular values, therefore problems with parameterization of $\langle S_Z\rangle_{Ln}$ and C_{Ln} just cannot arise, which makes it especially attractive for analysis of LIS arrays in wide range of experimental conditions. Applicability of this method in present studies is also justified by virtual equivalence of crystal-field parameters for two non-equivalent lanthanide ions [11].

$$\frac{\Delta\delta_l}{\Delta\delta_m} = \alpha_{klm} \cdot \frac{\Delta\delta_k}{\Delta\delta_m} + \beta_{klm} \tag{11}$$

$$\alpha_{klm} = \frac{F_l/F_m - G_l/G_m}{F_k/F_m - G_k/G_m} \tag{12}$$

$$\beta_{klm} = \frac{(F_l/F_m)\cdot(G_k/G_m) - (F_k/F_m)\cdot(G_k/G_m)}{F_k/F_m - G_k/G_m} \tag{13}$$

The coefficients α_{klm} and β_{klm} given by Eqs. (12) and (13) contain information about both structural characteristics and hyperfine coupling constants, however their nonlinear character precludes unambiguous assignment of possible breaks, which can be revealed by this technique. Therefore, simultaneous application of all possible methods is strongly recommended to perform analysis of LIS in terms of contact and dipolar contributions in order to reveal structural and electronic variations and to eliminate occasional compensation effects [27,28].

To perform the analysis, ten possible "*klm*" triads were selected in the same manner as described above. Performing this analysis for different triads "*klm*" of protons in [Pc*]M(Pc)M(Pc) systematically revealed that lanthanides split into two subfamilies, but in the present case the position of border is less evident then in the case of one nucleus technique.

While the "heavy" subfamily, namely (Dy–Tm), is characterized by perfect regression coefficients, the "light" group (Nd–Tb) demonstrates more scattered data. Surprisingly, further detailed examination of all ten three nuclei plots reveals that in all cases Tb almost equally can be attributed to "light" and "heavy" subfamilies. It becomes apparent due to the fact that transferring of Tb from the former to the later group doesn't lead to any significant decrease of R^2 values; neither, strong perturbations of α_{klm} and β_{klm} are observed. To the contrary, in the case of "light" subfamily removal of Tb leads to some increase of R^2 and stronger variations of regression coefficients. Altogether, this evidences that in the course of three nuclei analysis Tb behaves more like "heavy" lanthanide in contradiction with the results, obtained in the course of one nucleus analysis.

To make the partitioning (Nd–Eu)(Tb–Tm) more evident, we took the fourth nucleus for consideration and made 3D-plots in coordinates $(\Delta\delta_k/\Delta\delta_n; \Delta\delta_l/\Delta\delta_n; \Delta\delta_m/\Delta\delta_n)$. Performing multiple linear regressions for two subfamilies – (Tb–Tm) and (Dy–Tm) result in almost equal regression coefficients, supporting that Tb behaves as a "heavy" element in course of three nuclei analysis. To the contrary, addition of Tb to "light" lanthanides results in significant variations of multiple regression coefficients. The projections of these points onto the *xy*-, *xz*- and *yz*-planes are traditional three nuclei plots, which are obtained in 2D-coordinate systems (Fig. 6).

Since the coefficients of three nuclei method contain information about geometry and hyperfine coupling constants, variations of any or both of these factors may result in discontinuity of α_{klm} and β_{klm}. The possibility of abrupt geometrical variations already has been excluded via two nuclei analysis. Therefore, the observed partitioning (Nd–Eu)(Tb–Tm) evidences that the variation of F_k occurs actually between Eu and Tb, but not between Tb and Dy, as was previously supposed from the results of one nucleus analysis, while crystal-field parameter $A_2^0\langle r^2\rangle$ still undergoes abrupt change between Tb and Dy.

We have revisited Willcott agreement factors AF_{Ln}, Eq. (14) which were used to estimate the quality of LIS simulations in subfamilies (Nd–Tb) and (Nd–Eu) with the application of terms, obtained in the course of one nucleus analysis.

$$AF_{\mathrm{Ln}} = \sqrt{\frac{\sum_k \left(\Delta\delta^{obs}_{k,\mathrm{Ln}} - \Delta\delta^{calc}_{k,\mathrm{Ln}}\right)^2}{\sum_k \left(\Delta\delta^{obs}_{k,\mathrm{Ln}}\right)^2}} \tag{14}$$

It can be clearly seen that AF_{Ln} for "light" and "heavy" subfamilies are highly sensitive to inclusion or exclusion of Tb (Fig. 7). Both subfamilies (Nd–Tb) and (Tb–Tm) are characterized by larger AF_{Ln} values in comparison with groups (Nd–Eu) and (Dy–Tm), which do not contain Tb. However, LIS of Tb complex can be finely simulated when F_k is taken from (Dy–Tm) analysis and $A_2^0\langle r^2\rangle$ – from (Nd–Tb) data. Such a combination of these terms for simula-

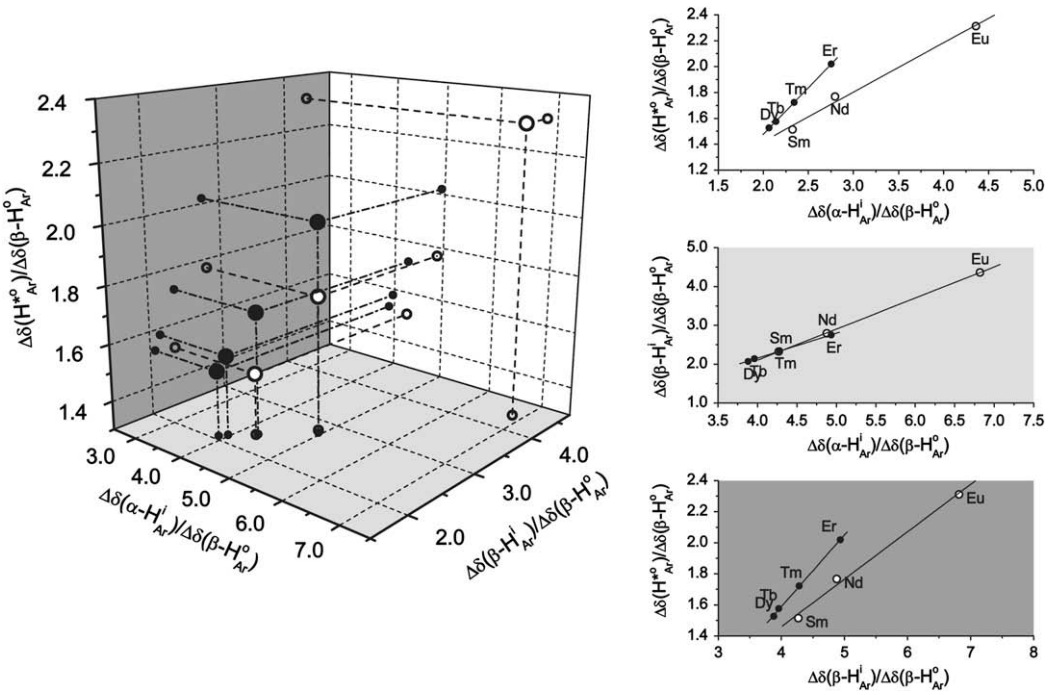

Fig. 6. 3D plot $\left(\frac{\Delta\delta(\alpha\text{-}H^i_{Ar})}{\Delta\delta(\beta\text{-}H^o_{Ar})}; \frac{\Delta\delta(\beta\text{-}H^i_{Ar})}{\Delta\delta(\beta\text{-}H^o_{Ar})}; \frac{\Delta\delta(H^{*o}_{Ar})}{\Delta\delta(\beta\text{-}H^o_{Ar})}\right)$ and its projections onto coordinate *xy*-, *xz*- and *yz*-planes. Open circles define "light" lanthanides (Nd–Eu) and closed – "heavy" elements (Tb–Tm).

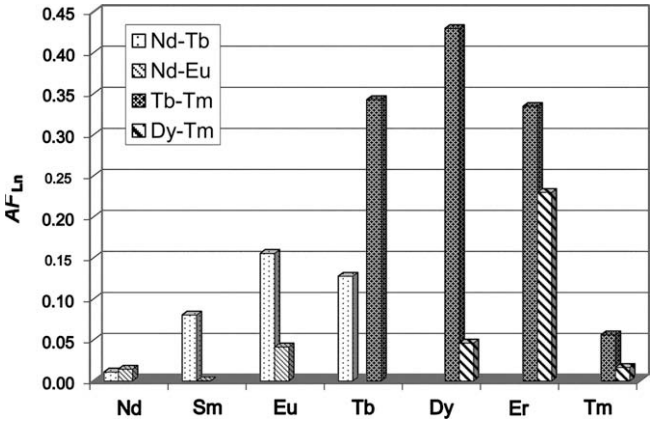

Fig. 7. Agreement factors AF_{Ln} for lanthanides, obtained in the course of simulation of LIS with the data, available from one nucleus analysis.

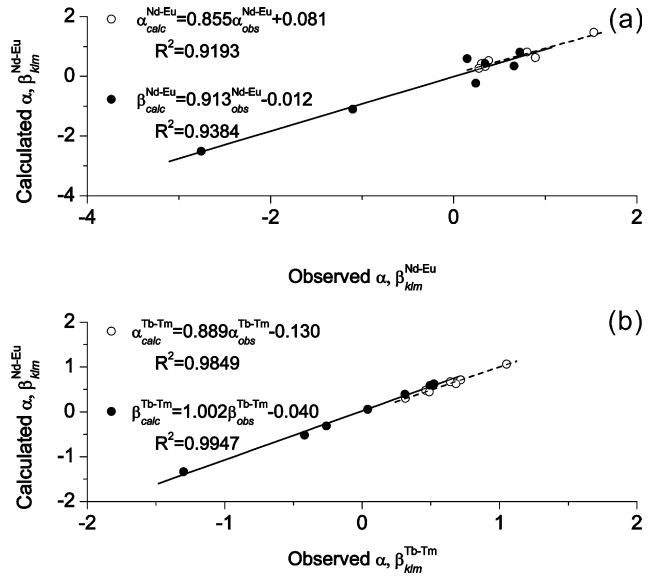

Fig. 8. Correlations between observed and calculated α_{klm} and β_{klm} for (Nd–Eu) and (Tb–Tm).

tion of LIS in Tb complex afforded $AF_{Ln} = 0.03$ therefore supporting the hypothesis of change of F_k between Eu and Tb rather than between Tb and Dy.

Since the refined contact and dipolar terms became available (Tables 2 and 3), we could use them to simulate the observed α_{klm} and β_{klm} values to check the validity of the proposed model. As a result of such simulation, both groups – (Nd–Eu) and (Tb–Tm) exhibited good correlation between experimental and calculated coefficients α_{klm} and β_{klm} (Fig. 8), the only mismatch was observed only in cases of triads with small regression coefficients ($R^2 < 0.82$). The observed satisfactory fit between observed and simulated α_{klm} and β_{klm} generally supports the model of non-simultaneous variation of F_k and $A_2^0\langle r^2\rangle$.

4. Conclusion

Simultaneous one- and multinuclei analysis of LIS values in series of triple-decker heteroleptic lanthanide crownphthalocyaninates $[(15C5)_4Pc]M(Pc)M(Pc)$ was firstly performed to determine the applicability domain of each method in the case of complexes with structurally non-equivalent lanthanide ions.

Separation of LIS values to contact and dipolar contributions by one nucleus analysis demonstrated abrupt changes of contact and dipolar terms $^{\Sigma}F_k$ and $^{\Sigma}A_2^0\langle r^2\rangle \cdot G_k$ near the middle of lanthanide series, which split these elements into two subfamilies, namely (Nd–Tb) and (Dy–Tm).

Crystal-field independent 3D-plots $(\Delta\delta_k/\langle S_Z\rangle;\Delta\delta_l/\langle S_Z\rangle;\Delta\delta_m/\langle S_Z\rangle)$ [21] (Eqs. (7)–(10)) let us exclude possible gross geometrical variations, therefore evidencing that the terms $^{\Sigma}A_2^0\langle r^2\rangle \cdot G_k$ change occurs because of solely variation of crystal-field second-rank terms $A_2^0\langle r^2\rangle$.

The same conclusion was drawn via application of crystal-field free 2D plots $(\Delta\delta_k/\langle S_Z\rangle;\Delta\delta_l/\langle S_Z\rangle)$ (Eq. (6)). Applicability of this approach was proved by analysis of previously reported values of crystal-field parameters of heteroleptic heteronuclear trisphthalocyaninates [11].

Behavior of F_k was studied via three nuclei plots $(\Delta\delta_k/\Delta\delta_m;\Delta\delta_l/\Delta\delta_m)$ [27] (Eqs.)(11)–(13)). This method yielded another partition in comparison with one nucleus technique, namely (Nd–Eu) and (Tb–Tm). Contradictory partitioning of lanthanides was explained by non-simultaneous variations of contact and dipolar terms, namely F_k undergoes abrupt changes between Eu and Tb while $A_2^0\langle r^2\rangle$ – between Tb and Dy. This explanation let us refine values of $^{\Sigma}F_k$ and $^{\Sigma}A_2^0\langle r^2\rangle \cdot G_k$ to get excellent fit between experimental and simulated values of LIS.

Validation of applicability of Eq. (6) let us refine geometrical characteristics of complexes in solution, which are well suited for the building of structural models of crown-substituted trisphthalocyaninates and their supramolecular assemblies in solution.

Acknowledgements

This work was supported by the Russian Foundation for Basic Research (Grants # 07-03-13547, 07-03-92212 and 08-03-00835), Russian Academy of Science Programs, European Research Association "Suprachem" and by International Science and Technology Center (Grant # 3718).

Appendix A. Supplementary data

Supplementary data associated with this article can be found, in the online version, at doi:10.1016/j.poly.2009.06.009.

References

[1] (a) J.-C.G. Bünzli, Acc. Chem. Res. 39 (2006) 53;
(b) S.P. Fricker, Chem. Soc. Rev. 35 (2006) 524;
(c) C.M.G. dos Santos, A.J. Harte, S.J. Quinn, T. Gunnlaugsson, Coord. Chem. Rev. 23–24 (2008) 2512.
[2] (a) C. Piguet, C.F.G.C. Geraldes, in: K.A. Gschneidner Jr., J.-C.G. Bünzli, V.K. Pecharsky (Eds.), Handbook on the Physics and Chemistry of Rare Earths, vol. 3, North-Holland Publishing Company, Amsterdam, 2003, p. 353;
(b) A.F. Cockerill, G.L.O. Davies, R.C. Harden, D.M. Rackham, Chem. Rev. 73 (1973) 553;
(c) J.A. Peters, J. Huskens, D.J. Raber, Prog. NMR Spectrosc. 28 (1996) 382;
(d) L. Di Bari, P. Salvadori, Coord. Chem. Rev. 249 (2005) 2854;
(e) C.F.G.C. Geraldes, S. Zhang, A.D. Sherry, Bioinorg. Chem. Appl. 1 (2003) 1;
(f) C.F.G.C. Geraldes, S. Zhang, A.D. Sherry, Inorg. Chim. Acta 357 (2004) 381;
(g) G. Pintacuda, M. John, X.-C. Su, G. Otting, Acc. Chem. Res. 40 (2007) 206;
(h) S.P. Babailov, Prog. Nucl. Magn. Reson. 52 (2008) 1.
[3] (a) R.M. Golding, M.P. Halton, Aust. J. Chem. 25 (1972) 2577;
(b) A.A. Pinkerton, M. Rossier, S. Spiliadis, J. Magn. Reson. 25 (1985) 420.
[4] (a) B. Bleaney, J. Magn. Reson. 8 (1972) 91;
(b) R.M. Golding, P. Pyykko, Molec. Phys. 26 (1973) 1389;
(c) B.R. McGarvey, J. Magn. Reson. 33 (1979) 445.
[5] (a) J.W. Buchler, D.K.P. Ng, in: K.M. Kadish, K.M. Smith, G. Guilard (Eds.), The Porphyrin Handbook, vol. 3, Academic Press, 2000, p. 245;
(b) J. Jiang, K. Kasuga, D.P. Arnold, in: H.S. Nalwa (Ed.), Supramolecular Photosensitive and Electroactive Materials, Academic Press, 2001, p. 113;
(c) R. Weiss, J. Fischer, in: K.M. Kadish, K.M. Smith, G. Guilard (Eds.), The Porphyrin Handbook, vol. 16, Elsevier Science, 2003, p. 171;
(d) J. Jiang, D.K.P. Arnold, Acc. Chem. Res. 42 (2009) 79.
[6] (a) R. Rosseau, R. Aroca, M.L. Rodriguez-Mendez, J. Mol. Struct. 356 (1995) 49;
(b) P. Zhu, N. Pan, C. Ma, X. Sun, D.P. Arnold, J. Jiang, Eur. J. Inorg. Chem. (2004) 518.

[7] (a) J.W. Buchler, M. Kihn-Botulinski, J. Loffler, M. Wicholas, Inorg. Chem. 28 (1989) 3770;
(b) J.W. Buchler, J. Loffler, M. Wicholas, Inorg. Chem. 31 (1992) 524.
[8] H. Konami, M. Hatano, A. Tajiri, Chem. Phys. Lett. 160 (1989) 163.
[9] N. Ishikawa, M. Sugita, T. Okubo, N. Tanaka, T. Iino, Y. Kaizu, Inorg. Chem. 42 (2003) 2440.
[10] D.P. Arnold, J. Jiang, J. Phys. Chem. A 105 (2001) 7525.
[11] (a) N. Ishikawa, T. Iino, Y. Kaizu, J. Phys. Chem. A 106 (2002) 9543;
(b) N. Ishikawa, T. Iino, Y. Kaizu, J. Am. Chem. Soc. 124 (2002) 11440;
(c) N. Ishikawa, T. Iino, Y. Kaizu, J. Phys. Chem. A 107 (2003) 7879.
[12] A.G. Martynov, O.V. Zubareva, Yu.G. Gorbunova, S.G. Sakharov, S.E. Nefedov, F.M. Dolgushin, A. Yu. Tsivadze, Eur. J. Inorg. Chem. (2007) 4800.
[13] A.G. Martynov, O.V. Zubareva, Yu.G. Gorbunova, S.G. Sakharov, A.Yu. Tsivadze, Inorg. Chim. Acta 362 (2009) 11.
[14] (a) N. Kobayashi, A.B.P. Lever, J. Am. Chem. Soc. 109 (1987) 7433;
(b) O.E. Sielcken, M.M. van Tilborg, M.F.M. Roks, R. Hendriks, W. Drenth, R.J.M. Nolte, J. Am. Chem. Soc. 109 (1987) 4261;
(c) V. Ahsen, E. Yilmazer, M. Ertas, O. Bekaroglu, J. Chem. Soc., Dalton Trans. (1988) 401;
(d) Y.G. Gorbunova, L.A. Lapkina, A.Yu. Tsivadze, J. Coord. Chem. 56 (2003) 1223;
(e) N. Ishikawa, Y. Kaisu, Coord. Chem. Rev. 226 (2002) 93;
(f) A.Yu. Tsivadze, Russ. Chem. Rev. 73 (2004) 5;
(g) N. Sheng, R. Li, C.-F. Choi, W. Su, D.K.P. Ng, X. Cui, K. Yoshida, N. Kobayashi, J. Jiang, Inorg. Chem. 45 (2006) 3794;
(h) A.G. Martynov, Yu.G. Gorbunova, Inorg. Chim. Acta 360 (2007) 122.
[15] (a) T. Toupance, V. Ahsen, J. Simon, J. Am. Chem. Soc. 116 (1994) 5352;
(b) T. Toupance, H. Benoit, D. Sarazin, J. Simon, J. Am. Chem. Soc. 119 (1997) 9191;
(c) T. Thami, C. Chassenieux, C. Fretigny, J.-P. Roger, F. Steybe, J. Porphyrins Phthalocyanines 6 (2002) 563;
(d) Y. Chen, W. Su, M. Bai, J. Jiang, X. Li, Y. Liu, L. Wang, S. Wang, J. Am. Chem. Soc. 127 (2005) 15700;
(e) Y. Chen, R. Li, R. Wang, P. Ma, S. Dong, Y. Gao, X. Li, J. Jiang, Langmuir 23 (2007) 12549;
(f) A.D. Grishina, Y.G. Gorbunova, V.I. Zolotarevsky, L.Ya. Pereshivko, Y.Yu. Enakieva, T.V. Krivenko, V. Savelyev, A.V. Vannikov, A.Yu. Tsivadze, J. Porphyrins Phthalocyanines 13 (2009) 92.
[16] M.D. Kemple, B.D. Ray, K.B. Liprowitz, F.G. Prendergast, B.D. Nageswara Rao, J. Am. Chem. Soc. 25 (1988) 8275.
[17] (a) C.N. Reilley, B.W. Good, J.F. Desreux, Anal. Chem. 47 (1975) 2110;
(b) C.N. Reilley, B.W. Good, R.D. Allendoerfer, Anal. Chem. 48 (1976) 1446.
[18] S. Rigault, C. Piguet, J. Am. Chem. Soc. 122 (2000) 9304.
[19] J.A. Peters, J. Magn. Reson. 68 (1986) 241.
[20] (a) M. Elhabiri, R. Scopelliti, J.-C.G. Bu1nzli, C. Piguet, J. Am. Chem. Soc. 121 (1999) 10747;
(b) S. Rigault, C. Piguet, J.-C.G. Bunzli, J. Chem. Soc., Dalton Trans. (2000) 2045;
(c) N. Ouali, J.-P. Rivera, P.-Y. Morgantini, J. Weber, C. Piguet, Dalton Trans. (2003) 1251.
[21] (a) N. Ouali, J.-P. Rivera, P. Delange, C. Piguet, Inorg. Chem. 43 (2004) 1517;
(b) E. Terazzi, J.-P. Rivera, N. Ouali, C. Piguet, Magn. Reson. Chem. 44 (2006) 539.
[22] Y. Bian, L. Li, D. Wang, C.-F. Choi, D.Y.Y. Cheng, P. Zhu, R. Li, J. Dou, R. Wang, N. Pan, D.K.P. Ng, N. Kobayashi, J. Jiang, Eur. J. Inorg. Chem. (2005) 2612.
[23] (a) M.R. Willcott III, R.E. Lenkinski, R.E. Davis, J. Am. Chem. Soc. 94 (1972) 1742;
(b) R.E. Davis, M.R. Willcott III, J. Am. Chem. Soc. 94 (1972) 1744.
[24] J. Reuben, J. Magn. Reson. 50 (1982) 233.
[25] C. Platas, F. Avecilla, A. de Blas, C.F.G.C. Geraldes, T. Rodrguez-Blas, H. Adams, J. Maha, Inorg. Chem. 38 (1999) 3190.
[26] (a) H. Huckstadt, A. Tutass, M. Goldner, U. Cornelissen, H. Homborg, Z. Anorg. Allg. Chem. 627 (2001) 485;
(b) Y. Bian, D. Wang, R. Wang, L. Weng, J. Dou, D. Zhao, D.K.P. Ng, J. Jiang, New J. Chem. 27 (2003) 844.
[27] C.F.G.C. Geraldes, S. Zhang, C. Platas, T. Rodriguez-Blas, A. de Blas, A.D. Sherry, J. Alloys Compd. 323-324 (2001) 824.
[28] N. Ouali, B. Bocquet, S. Rigault, P.-Y. Morgantini, J. Weber, C. Piguet, Inorg. Chem. 41 (2002) 1436.